THE ASTROPHYSICAL JOURNAL, 486:L5–L9, 1997 September 1
© 1997. The American Astronomical Society. All rights reserved. Printed in U.S.A.

RADIO AND OPTICAL FOLLOW-UP OBSERVATIONS AND IMPROVED INTERPLANETARY NETWORK POSITION OF GRB 970111

T. J. GALAMA,[1] P. J. GROOT,[1] R. G. STROM,[1,2] J. VAN PARADIJS,[1,3] K. HURLEY,[4] C. KOUVELIOTOU,[5,6] G. J. FISHMAN,[6] C. A. MEEGAN,[6] J. HEISE,[7] J. J. M. IN'T ZAND,[7] A. G. DE BRUYN,[2,8] L. O. HANLON,[9] K. BENNETT,[10] J. H. TELTING,[11] AND R. G. M. RUTTEN[11]

Received 1997 February 7; accepted 1997 June 12

ABSTRACT

We report on Westerbork 840 MHz and 1.4 and 5 GHz radio observations of the improved Interplanetary Network Wide Field Camera (IPN WFC) error box of the γ-ray burst GRB 970111, between 26.4 hr and 120 days after the event onset. In the $\sim$13 arcmin^2 area defined by the IPN (BATSE and *Ulysses*) annulus and the published refined *BeppoSAX* WFC error box, we detected no steady sources brighter than 0.56 mJy (4 σ) and no varying radio emission, down to 1.0 mJy (4 σ). We also report on *B*-, *V*-, *R*-, and *I*-band observations of the error box with the 4.2 m William Herschel Telescope at La Palma.

Subject headings: gamma rays: bursts — radio continuum: general

1. INTRODUCTION

The isotropic and inhomogeneous distribution of γ-ray bursts (GRBs) (Meegan et al. 1992; Briggs et al. 1996) is explained in a natural way if GRB sources are located at cosmological distances on the order of gigaparsecs (Usov & Chibisov 1975; Paczyński 1986; Goodman 1986; Fenimore et al. 1993). However, a GRB source distribution in a very large galactic halo (characteristic size, 10^5 pc) is also advocated (see, e.g., Podsiadlowki, Rees, & Ruderman 1995). Independent of what the distance scale of GRB sources is, the mechanism that gives rise to the sudden emission of γ rays is unknown, and it is generally believed that progress in solving this problem requires the detection of GRB counterparts in other parts of the electromagnetic spectrum. Very promising in providing new insights of the origin and production mechanism of GRBs are the recent discovery of an optical transient related to GRB 970228 (Van Paradijs et al. 1997; Groot et al. 1997a) and the monitoring of its optical light curve (Galama et al. 1997a; Sahu et al. 1997). The optical transient may be associated with a faint galaxy (Van Paradijs et al. 1997; Groot et al. 1997b), which suggests that it lies at a cosmological distance.

The peak luminosities of GRBs are highly super-Eddington, even for galactic halo models. Paczyński & Rhoads (1993) pointed out that it is hard to avoid relativistic outflows from the GRB source and that the interaction of these flows with an interstellar medium must generate radio emission, as observed, e.g., in extragalactic jet sources (see also Katz 1994b; Mészáros, Rees, & Papathanassiou 1994; Mészáros & Rees 1997). Paczyński & Rhoads estimated that the strongest GRBs may be followed by transient ($\sim$20 mJy) radio emission at intervals ranging from minutes (for the galactic halo distance scale) to roughly weeks to months (for the cosmological distance scale).

We report here on observations of the refined error box of GRB 970111 (in't Zand et al. 1997) made with the Westerbork Synthesis Radio Telescope (WSRT) in the months following the burst and the derivation of a substantially improved Interplanetary Network (IPN) error box based on the time delay between the burst as observed with the Burst and Transient Source Experiment (BATSE) and *Ulysses*. In § 2 we describe the properties of the GRB as observed with BATSE and present the IPN-*BeppoSAX* error box. In § 3 we describe the radio and optical observations, the results of which are discussed in § 4.

2. GRB 970111 Γ-RAY OBSERVATIONS

2.1. *BATSE Observations*

GRB 970111 triggered BATSE on 1997 January 11 at 09:44:00 UT. Here we describe data obtained with the Large Area Detectors (LADs); a detailed description of the instrument is given elsewhere (Fishman et al. 1989). Figure 1 shows the burst profile (with 1.024 s time resolution) in four energy channels (25–50, 50–100, 100–300, and >300 keV). The event duration is T_{90} = 31.7 s, estimated from the summed signals of all energy channels (T_{90} is the time during which 90% of the total burst counts are emitted; Kouveliotou et al. 1993).

When we fit a broken power law to the event energy spectrum, we find that the total 25 keV–1.8 MeV fluence during 48.4 s of emission is $5.8 \pm 0.3 \times 10^{-5}$ ergs cm^{-2}. This fluence is among the top 1% of all GRBs observed with BATSE so far. The event peak flux (summed over the same energy range in 1.024 s intervals) is $4.4 \pm 0.2 \times 10^{-6}$ ergs cm^{-2} s^{-1}, which makes GRB 970111 one of the top 5% brightest BATSE events. A slightly better fit is obtained with the Band

[1] Astronomical Institute Anton Pannekoek, University of Amsterdam, and Center for High Energy Astrophysics, Kruislaan 403, 1098 SJ Amsterdam, The Netherlands.
[2] Netherlands Foundation for Radio Astronomy (NFRA), Postbus 2, 7990 AA Dwingeloo, The Netherlands.
[3] Department of Physics, University of Alabama in Huntsville, Huntsville, AL 35899.
[4] Space Sciences Laboratory, Berkeley, CA 94720-7450.
[5] Universities Space Research Association.
[6] NASA/Marshall Space Flight Center, Code ES-84, Huntsville, AL 35812.
[7] Space Research Organization Netherlands, Sorbonnelaan 2, 3584 CA Utrecht, The Netherlands.
[8] Kapteyn Astronomical Institute, Postbus 800, 9700 AV, Groningen, The Netherlands.
[9] Department of Physics, University College Dublin, Belfield, Dublin 4, Ireland.
[10] Astrophysics Division, Space Science Department, European Space Research and Technology Center, Noordwijk, The Netherlands.
[11] ING Telescopes/NFRA, Apartado 321, Santa Cruz de La Palma, Tenerife 38780, Spain.

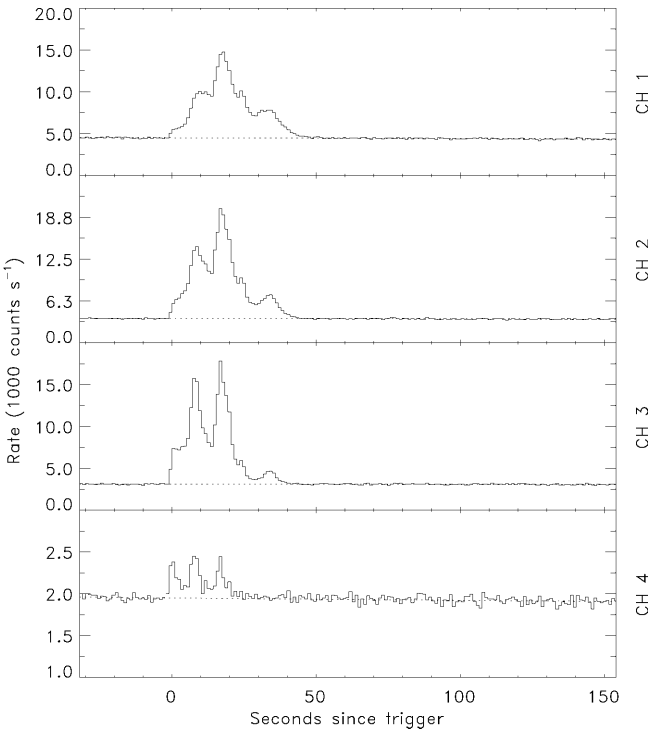

FIG. 1.—BATSE light curve of GRB 970111 in the four LAD energy channels, 25–50, 50–100, 100–300, and >300 keV (channel 1 being that of the lowest energy). Time resolution is 1.024 s.

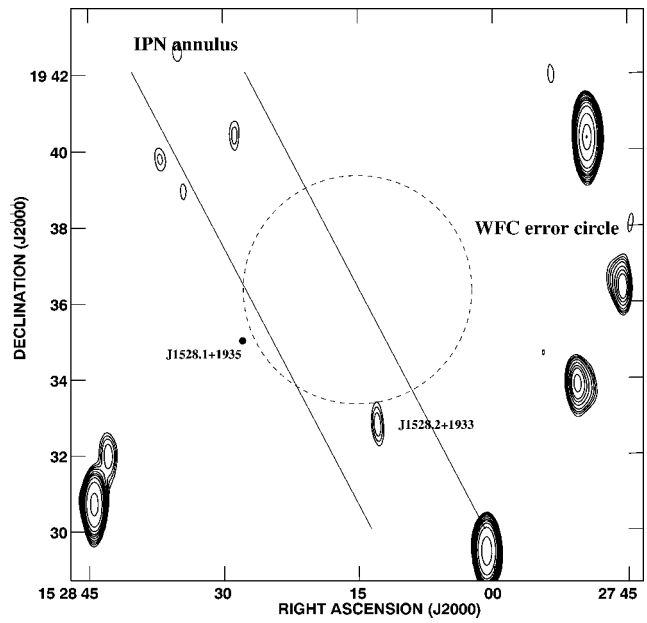

FIG. 2.—Contour plot of the WSRT 840 MHz image of GRB 970111 field centered at the refined WFC position $\alpha = 15^h28^m15^s$, $\delta = +19°36'18''$ (equinox J2000). Combined are data from January 13, 14, 16, 20, and 29 and March 9. Included are the refined WFC 3′ radius error region (3 σ) and the refined 3 σ *Ulysses*-BATSE triangulation annulus. Indicated are the radio source J1528.2+1933 and the position of the radio source J1528.1+1933 (*filled circle*), both located just outside the WFC error box. Contour levels are 0.56, 0.70, 0.84, 1.05, 1.40, 1.75, 2.10, 2.80, 4.20, 8.40, 16.80, and 22.25 mJy (0.14 mJy noise).

function (Band et al. 1993), for which we find that the spectral power peaks at $E_{peak} = 166 \pm 1$ keV.

In the burst profile summed over all channels, we distinguish five peaks: channel 4 shows only the first three, and channel 1 shows only the last four. The peaks occur at times (since trigger) $T \sim 1$ s, ~8 s, ~17 s, ~25 s, and ~35 s. Thus, this event shows strong spectral evolution, with the first peak having a very hard spectrum starting above ~100 keV and the last two having much softer spectra. This is confirmed in the *BeppoSAX* Wide Field Camera observations (WFC; energy range 1.8–30 keV), in which there are only two peaks, which start ~20 and ~35 s, respectively, after the BATSE trigger time. Spectral evolution in GRBs is well known; GRB 970111 is an extreme example of late pulses disappearing entirely at high energies (see Ford et al. 1995 for a detailed description of spectral evolution trends of bursts observed with BATSE).

The burst location, found with the directional response of the BATSE detectors that recorded the burst, was $\alpha = 231°$ and $\delta = 19°$ (J2000) with a total error of 1°.5 (statistical and systematic added in quadrature). Fortunately, besides the two near-Earth satellites *Compton Gamma Ray Observatory* (*CGRO*) and *BeppoSAX*, the event was also recorded with the *Ulysses* spacecraft, which allowed the derivation of a very narrow and short IPN annulus (see Hurley et al. 1994 for a description of IPN error boxes).

2.2. *IPN BeppoSAX WFC Combined Error Box*

Triangulation of this event using *Ulysses* and BATSE data gives an annulus of possible arrival directions. This annulus is centered at $\alpha = 11^h50^m55^s.4$, δ +33°21′57″ (J2000) and has a radius of 49°.983 ± 0°.022 (3 σ confidence). It is consistent with the one given by Hurley et al. (1997), but narrower. Combining this annulus with the refined *BeppoSAX* WFC error circle (in't Zand et al. 1997) gives an approximately trapezoidal error box whose corners are at $\alpha = 15^h28^m22^s$, $\delta = +19°33'45''$; $\alpha = 15^h28^m28^s$, $\delta = +19°36'28''$; $\alpha = 15^h28^m09^s$, $\delta = +19°33'40''$; and $\alpha = 15^h28^m21^s$, $\delta = +19°38'59''$ (J2000) and whose area is approximately 13 arcmin^2 (see Fig. 2). Of the three *BeppoSAX* and *ROSAT* quiescent soft X-ray sources (Butler et al. 1997; Voges, Boller, & Greiner 1997) found in the preliminary WFC error circle (Costa et al. 1997), none lie within this error box.

3. RADIO AND OPTICAL OBSERVATIONS

3.1. *Radio Observations*

The error box of GRB 970111 was first observed at 840 MHz with the WSRT at the preliminary position given by Costa et al. (1997) on January 12, at UT 12:51, starting 26.4 hr after the event, for only 1.44 hr until the GRB source exceeded the telescope hour-angle limit. Subsequent 12 hr observations were made on January 13.31, 14.31, 16.31, 20.30 and 29.27, March 9.16, and April 9.08 (where the notation refers to the day and the fraction of the day; these and subsequent observing times refer to the middle of the observing period).

We used a new UHF receiving system whose upper frequency band covers the 700–1200 MHz range and selected 840 MHz because electromagnetic interference (EMI) is usually absent there. The standard continuum correlator was used, providing us with eight contiguous 10 MHz bands from 800 to 880 MHz. The noise level in a continuum map for a 10 MHz bandwidth after 12 hr of integration is typically 0.5 mJy beam^{-1}, and our analysis shows that this was usually achieved in the present series of measurements. At 840 MHz, the

synthesized beamwidth at 20° declination is 21″ × 62″ (R.A. × decl.), and the field of view (half-power beamwidth) is about 1°.

We also observed at 5 GHz on February 26.05 (5.15 hr) and 27.29 (5.55 hr) and March 2.22 (10.24 hr). With eight bands of 10 MHz width each, we obtained noise levels of ~0.15 mJy per observation. The synthesized beamwidth at 20° declination is 6″ × 18″ (R.A. × decl.). The field of view (half-power beamwidth) is about 0°.17.

The latest observations were for 8.4 hr each at 1.4 GHz on May 11.07 and 12.06 (120.6 days after the event). The 1.4 GHz data consist of five bands of 10 MHz width (two were bad) and three bands of 5 MHz width, which provided a useful 45 MHz of bandwidth. The noise level combining the two 1.4 GHz observations is 0.070 mJy. The synthesized beamwidth at 20° declination at 1.4 GHz is 13″ × 37″ (R.A. × decl.). The field of view (half-power beamwidth) is about 0°.6.

The data were analyzed with the NEWSTAR software package. The interferometer complex visibilities were first examined for possible EMI and other obvious defects. Bands with strong interference were either deleted or carefully edited. Because of interference, about 45% of the data were unusable in the January 14 observation. On the other days, interference was usually limited to about 10%. In the self-calibration (gains and phases) we used models for the eight bands around 840 MHz, each containing nearly 80 discrete sources above 2.5 mJy. For calibration of interferometer gain and phase, for each observation and each band, we used the standard WSRT calibrator 3C 48 (24.05 Jy at 840 MHz, 15.96 Jy at 1.4 GHz, and 5.55 Jy at 5 GHz; based on the 3C286 flux density on the Baars et al. 1977 scale). The 840 MHz map of the field produced by combining data from January 13, 14, 16 20, and 29 and March 9 is shown in Figure 2. The 1.4 GHz observations have been analyzed in a similar way, but no self-calibration was performed. The 5 GHz observations contained only very weak sources within the field of view, and hence no model has been obtained and no self-calibration was performed.

We searched for a transient radio counterpart by looking for variability at 840 MHz within the refined WFC-*Ulysses*-BATSE error region. Since all our observations were obtained with the configurations of the Westerbork array, the synthesized beams of the images for different days are in principle the same. The most sensitive way to look for variations in the data is via the construction of difference maps from residual maps, i.e., maps deconvolved with a model containing all real sources in the field. We obtained equal synthesized beams in the residual maps of two observations by retaining only those $u - v$ points common to the data sets of any 2 days in the comparison. Subsequently, we subtracted the two maps from each other and obtained the difference map. In these difference maps we did not detect any source variation in the 13 arcmin^2 error box of GRB 970111, down to 1.0 mJy (4 σ), for the period 26.4 hr to 88 days after the burst, and down to 2.4 mJy (4 σ) for the first observation (January 12; see Fig. 3).

Since no radio source is found in the error box at any of the observing frequencies (840 MHz and 1.4 and 5 GHz), the 1.4 and 5 GHz upper limits to variability have been determined by considering the limit for detection of a radio source (for which we take 4 σ, which corresponds to 0.28 mJy at 1.4 GHz and 0.6 mJy at 5 GHz; see Fig. 3).

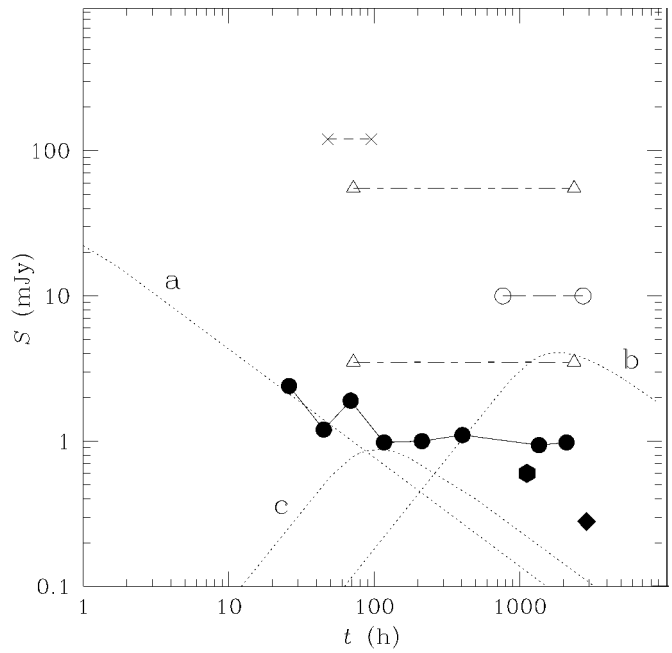

FIG. 3.—Log-log plot of the upper limits to variable radio emission from GRB 970111 (*filled symbols*) and GRB 940301 (*crosses and open symbols*) as a function of elapsed time since the γ-ray burst. The flux density limits at 840 MHz (*filled circles*) are from the eight WSRT observations discussed in this Letter (GRB 970111). The other limits are for 1.4 GHz (*filled diamond*) and 5 GHz (*filled hexagon*). The remaining measurements all refer to GRB 940301, at 151 MHz (Koranyi et al. 1995; *crosses*), 327 MHz (Galama et al. 1997c; *open circles*), 408 MHz (*upper open triangle*), and 1400 MHz (*lower open triangle*; Frail et al. 1994), all being upper limits to candidate sources in two or more observations over the time span indicated by the horizontal lines. The three dotted curves show the expected radio emission at 840 MHz from a γ-ray burst with a fluence of 5.8×10^{-5}ergs cm^{-2} according to the calculations of Paczyński & Rhoads (1993). Curve a is for a distance of 100 kpc (and peaks at 34 mJy after t = 22 minutes); curve b is for 0.5 Gpc, both for nominal values of ambient density, $\rho = 10^{-24}$g cm^{-3}, and efficiency, $\xi = 0.1$ (see text). Curve c is for 0.5 Gpc, with $\rho = 1.0 \times 10^{-26}$g cm^{-3} and $\xi = 0.3$.

3.2. *Optical Observations*

We made *B*-, *V*-, *R*-, and *I*-band images of the refined error box of GRB 970111 using the 4.2 m William Herschel Telescope (prime focus) on La Palma in service time. On February 28.2 UT, *B*, *V*, and *I* images were obtained with integration times of 930, 405, and 695 s, respectively, and an *R* image (405 s) was obtained on March 1.1 UT. The field of view is 7′.2 × 7′.2. Figure 4 (Plate L1) shows a *V*-band image of the region covering the WFC error box of GRB 970111. We made *B*-, *V*-, and *I*-magnitude calibrations with images of the photometric Landolt standard field 107 using stars 599–602. For the *R*-magnitude calibration we used Landolt standard field 104, stars 334, 336, 338, and 339. Comparison with the Digital Sky Survey shows no brightening of sources to $V = 19$. The two radio sources located near the error box (§ 4) show no counterpart down to $B = 23.7$, $V = 24.0$, $R = 22.9$, and $I = 21.7$. The combined GRB error box contains a few galaxies above the detection limit. One is a relatively bright galaxy (see Fig. 3), at $\alpha = 15^h28^m15''.2$, $\delta = +19°35'55''$ (equinox 2000.0), with $V = 20.2 \pm 0.1$, $B - V = +1.3 \pm 0.1$, $V - R = +0.7 \pm 0.1$, and $V - I = +1.4 \pm 0.1$. This galaxy is not detected in the radio observations at 840 MHz (<0.42 mJy, 3 σ), 1.4 GHz (<0.21 mJy, 3 σ), or 5 GHz (<0.45 mJy, 3 σ).

4. DISCUSSION

Using the combined map based on observations made on 12, 13, 16, 20, and 29 January and March 9, we find no 840 MHz radio sources in the error box of GRB 970111 (see Fig. 2), down to the detection limit of 0.56 mJy (4 σ). The (4 σ) detection limits at 1.4 GHz and 5 GHz are 0.28 mJy and 0.6 mJy, respectively. (Note that the limits reported in § 3.1 refer to variability of any radio source in the error box.) Two sources lie just outside the error box at $\alpha = 15^h28^m12^s.8 \pm 0^s.1$, $\delta = +19°32'50'' \pm 4''$ (J1528.2+1933) and $\alpha = 15^h28^m04^s.9 \pm 0^s.1$, $\delta = +19°35'00'' \pm 2''$ (J1528.1+1935). The 840 MHz and 1.4 and 5 GHz fluxes are as follows: 1.13 ± 0.14 mJy, 0.275 ± 0.07 mJy, and <0.45 mJy (J1528.2+1933) and <0.42 mJy, <0.21 mJy, and 0.80 ± 0.15 mJy (J1528.1+1935) (upper limits are 3 σ). Source A reported by Galama et al. (1997b) appeared, after the final analysis of subsequent observations, to be a noise peak.

Previous follow-up radio observations have not led to the detection of a variable radio signal that is possibly correlated with a GRB (see, e.g., the recent review by Vrba 1996). The deepest radio follow-up at short intervals so far is that by Frail et al. (1994), who obtained 5 σ upper limits of 3.5 mJy to variability at 1.4 GHz, within 3–99 days of GRB 940301, from observations of the COMPTEL error box of this burst (Frail et al. 1994). Galama et al. (1997c) derived upper limits of 10 mJy to variability at 325 MHz during an interval of 1–3 months after GRB 940301. Our present results improve the response time of Frail et al. (1994) by a factor of ~3. A similar improvement has been reported by Frail et al. (1997a).

To interpret our null result, we take as a guideline the work of Paczyński & Rhoads, which is based on the idea that GRBs are caused by the interaction of a relativistically expanding fireball with the interstellar medium (with density $\rho = 10^{-24}\rho_{24}$ g cm^{-3}). From their results (see their eqs. [18b] and [19b]) we estimate, using a burst fluence $S = 5.8 \times 10^{-5}$ ergs cm^{-2} and an observing frequency of 840 MHz, that the peak radio flux F_{max} and the time t_{max} since the GRB when this peak is reached are given by $F_{max} \sim (4.1 \text{ mJy})\, d_{0.5}^{-1/4}\rho_{24}^{1/8}$ and $t_{max} \sim (75 \text{ days})\, d_{0.5}\rho_{24}^{1/2}$; here $d_{0.5}$ is the source distance in units of 0.5 Gpc. (In these estimates we have set several of the dimensionless constants occurring in these equations equal to unity.) During the rise of the radio transient, the flux increases with time t proportional to $t^{5/4}$; the decay goes as $t^{-3/4}$.

The model of Katz (1994a, 1994b) predicts an initial 840 MHz flux (simultaneous with the GRB, taken to emit 5.8×10^{-5} ergs cm^{-2} in ~30 s, over a 4×10^{19} Hz bandwidth centered at 4×10^{19} Hz) of ~1.3 μJy. This flux rises proportionally to $t^{4/5}$ until it reaches a peak, roughly 30 s × [840 MHz/(4×10^{19} Hz)]$^{-5/12}$ ~ 10 days later, ~5 mJy. Thus, the models of Paczyński & Rhoads and of Katz predict radio afterglows for GRB 970111 that are quite similar.

GRB 970111 was extremely strong: it was among the top 1% of BATSE bursts with respect to fluence and among the top 5% with respect to peak flux. In the cosmological model for GRBs, the turnover in the cumulative burst peak flux distribution occurs at redshift $z \sim 1$ (see, e.g., Fenimore et al. 1993). Since the luminosity distribution of observed bursts is not very broad (see, e.g., Horack, Emslie, & Meegan 1994; Ulmer, Wijers, & Fenimore 1995), this indicates that GRB 970111 originated at a rather modest redshift (of order 0.1). We will therefore, in the following, assume a nominal source distance of 0.5 Gpc.

In Figure 3 we have plotted our upper limits as a function of time since the burst, together with some of the best previous limits, and three curves showing the radio behavior according to the above expressions derived from the Paczyński & Rhoads model. It appears that our observations exclude the model of Paczyński & Rhoads at its nominal parameters (the same is the case for the Katz model). They suggest that for the model to be viable, GRB 970111 should have come either from very nearby (<20 kpc, peaking within a few minutes of the burst) or from a very large distance (>3 Gpc, with a peak after many months, in which case its peak luminosity would have been exceptionally high), or it occurred with a high efficiency of γ-ray production in regions of very low ambient density.

Although our nondetection of a radio counterpart for GRB 970111 nominally excludes the models of Paczyński & Rhoads (1993) and of Katz (1994a, 1994b), we feel that in both models there are enough scaling factors that disagreement by ~1 order of magnitude is not yet compelling evidence that the models are qualitatively wrong. Moreover, at low radio frequencies the emission may be limited by self-absorption (e.g., Katz 1994a).

After the revised version of this Letter was near completion, we learned of the detection of an optical and radio counterpart of GRB 970508 (Bond 1997; Frail et al. 1997b). The inverted spectrum $F_\nu \propto \nu^{+1.1}$ observed for this radio counterpart is evidence for the occurrence of self-absorption. The measurement of a redshift ($z > 0.835$, Metzger et al. 1997) of the optical counterpart of GRB 970508 may have settled the matter of the distance scale to GRB sources. It is clear that the relative response in the radio band is far from proportional to the strength of the GRB; the same is the case for the optical response (Castro-Tirado et al. 1997). It is currently unclear what GRB characteristic determines the low-energy response to GRBs, and more follow-up observations are required to unravel their systematics.

We will continue monitoring the error box of GRB 970111 in an attempt to detect any delayed radio signal from this event.

We are grateful for the assistance of the Westerbork Synthesis Radio Telescope (WSRT) operators G. Kuper and R. de Haan. The WSRT is operated by the Netherlands Foundation for Research in Astronomy (NFRA) with financial aid by the Netherlands Organization for Scientific Research. The William Herschel Telescope is operated on behalf of the Particle Physics and Astronomy Research Council (U.K.) and the NFRA at the Spanish observatory Roque de Los Muchachos on La Palma, Spain. T. Galama is supported through a grant from NFRA under contract 781.76.011. C. Kouveliotou acknowledges support from NASA grant NAG 5-2560. K. Hurley acknowledges support for *Ulysses* under JPL contract 958056, and for the Interplanetary Network under NASA grant NAG 5-1560.

REFERENCES

Baars, J. W. M., et al. 1977, A&A, 61, 99
Band, D., et al. 1993, ApJ, 413, 281
Bond, H. 1997, IAU Circ., 6654
Briggs, M. S., et al. 1996, ApJ, 459, 40
Butler, R. G., et al. 1997, IAU Circ., 6539
Castro-Tirado, A., et al. 1997, IAU Circ., 6598

Costa, E., et al. 1997, IAU Circ., 6533
Fenimore, E. E., et al. 1993, Nature, 366, 40
Fishman, G. J., et al. 1989, in Proc. GRO Sci. Workshop, ed. W. N. Johnson (Greenbelt: Goddard Space Flight Center), 3
Ford, L. A., et al. 1995, ApJ, 439, 307
Frail, D. A., et al. 1994, ApJ, 437, L43
———. 1997a, IAU Circ., 6545
———. 1997b, IAU Circ., 6662
Galama, T. J., et al. 1997a, Nature, 387, 479
———. 1997b, IAU Circ., 6571
———. 1997c, A&A, 321, 229
Goodman, J. 1986, ApJ, 308, 47
Groot, P. J., et al. 1997a, IAU Circ., 6584
———. 1997b, IAU Circ., 6588
Horack, J. M., Emslie, A. G., & Meegan, C. A. 1994, ApJ, 426, 5
Hurley, K., et al. 1994, in AIP Conf. Proc. 307, Gamma-Ray Bursts, ed. G. J. Fishman, J. J. Brainerd, & K. Hurley (New York: AIP), 27
———. 1997, IAU Circ., 6571
in't Zand, J., et al. 1997, IAU Circ., 6569
Katz, J. I. 1994a, ApJ, 422, 248
———. 1994b, ApJ, 432, L107
Koranyi, D. M., et al. 1995, MNRAS, 276, L13
Kouveliotou, C., et al. 1993, ApJ, 413, L101
Meegan, C. A., et al. 1992, Nature, 355, 143
Mészáros, P., & Rees, M. J. 1997, ApJ, 476, 232
Mészáros, P., Rees, M. J., & Papathanassiou, H. 1994, ApJ, 432, 181
Metzger, M., et al. 1997, IAU Circ., 6655
Paczyński, B. 1986, ApJ, 308, 43
Paczyński, B., & Rhoads, J. E. 1993, ApJ, 418, L5
Podsiadlowski, P., Rees, M. J., & Ruderman, M. 1995, MNRAS, 273, 755
Sahu, K. C., et al. 1997, Nature, 387, 476
Ulmer, A., Wijers, R. A. M. J., & Fenimore, E. E. 1995, ApJ, 440, 9
Usov, V. V., & Chibisov, G. V. 1975, Soviet Astron., 19, 115
Van Paradijs, J., et al. 1997, Nature, 386, 686
Voges, W., Boller, T., & Greiner, J. 1997, IAU Circ., 6539
Vrba, F. J. 1996, in AIP Conf. Proc. 384, Gamma-Ray Bursts, ed. C. Kouveliotou, M. F. Briggs, & G. J. Fishman (New York: AIP), 565

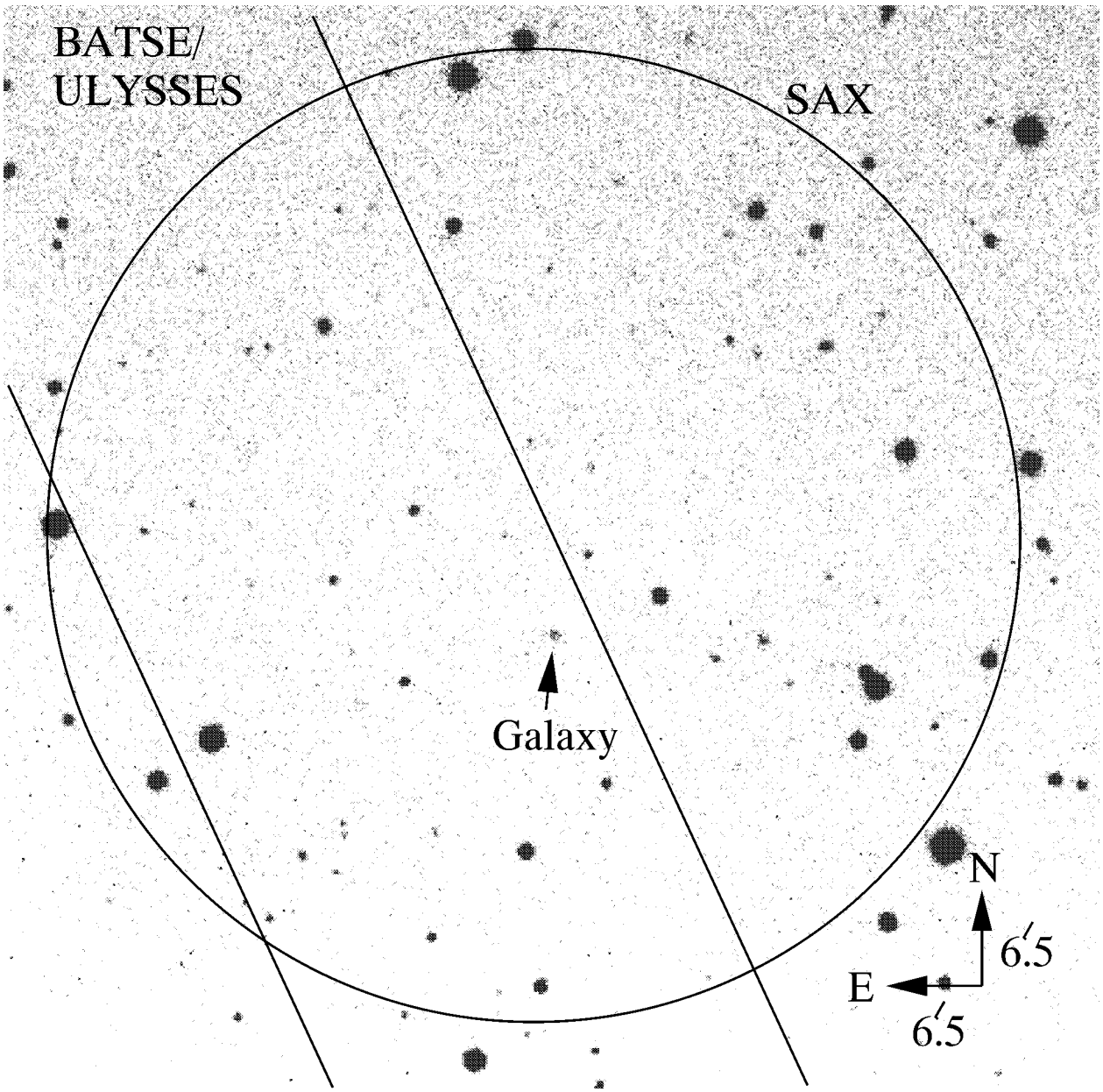

FIG. 4.—WHT prime focus *V*-band image of the field of GRB 970111. Indicated are the *BeppoSAX* WFC error circle, the IPN annulus, and the relatively bright galaxy mentioned in the text.

GALAMA et al. (see 486, L7)